JOURNAL OF CATALYSIS **170,** 123–131 (1997)
ARTICLE NO. CA971744

Preparation, Characterization, and Catalytic Behavior of Molybdenum Oxynitrides Supported on EMT Zeolite (NaEMT and HEMT) Catalysts

Thierry Bécue, Jean-Marie Manoli, Claude Potvin, and Gérald Djéga-Mariadassou[1]

Laboratoire Réactivité de Surface, URA CNRS 1106, Université P. & M. Curie, 4 Place Jussieu, 75252 Paris Cedex 05, France

Received September 27, 1996; revised April 9, 1997; accepted May 5, 1997

EMT zeolite-encaged molybdenum oxynitride clusters were prepared by several methods, leading to different dispersions of the molybdenum species. HRTEM and EDX measurements indicated that, when the molybdenum species were inside of the zeolite porosity, they were homogeneously dispersed in the form of clusters whose diameters were less than 10 Å. Depending on the preparation, it was shown by X-ray diffraction and specific surface area measurements that the EMT zeolite crystallinity was affected to different extents following ammonia treatments used for nitridation. The catalytic behavior of these nitrided compounds was studied in the *n*-heptane conversion. Supported on NaEMT, the encaged molybdenum oxynitride showed a reactivity of a bulk material. The most active catalyst was the low-temperature (523 K) catalyst, the *n*-heptane isomerization appearing as the main reaction. In contrast, for the catalysts supported on acidic HEMT, *n*-heptane cracking was mainly observed and the deactivation of the Mo-oxynitride supported catalysts was lowered compared to that of HEMT alone.

1. INTRODUCTION

Over the past two decades, there has been increasing interest in the transition metal carbides or nitrides due to their competitive activities for several reactions (1–5). Since many of these reactions were typically catalyzed by noble metals, the potential for using carbides and nitrides in such processes provided a strong motivation to explore the reactivity of these new intriguing materials and to prepare them with high specific surface areas (6–8).

These materials were pyrophoric; a passivation step was immediately carried out after nitridation. As a consequence these materials containing substantial amounts of oxygen were called molybdenum oxynitride (9). Due to the difficulty of preparing high-surface-area bulk materials, heterogeneous catalysts were typically prepared on high-surface-area supports and some promising results were reported. Nagai *et al.* (10) have shown that supported molybdenum nitrides on alumina are extremely active in the HDS of dibenzothiophene and in the HDN of carbazole (11), while Colling and Thompson have studied these compounds in the HDN of pyridine (12).

These results have encouraged the investigation of molybdenum oxynitrides supported on EMT zeolite, prepared by different loading methods (chemical vapor deposition, solid-state reaction, and incipient wetness impregnation) followed by a subsequent nitridation. The preparation and the characterization including the catalytic properties of these compounds for the *n*-heptane conversion are the objectives of this paper. The EMT zeolite is a hexagonal polytype of the Y cubic faujasite which has been recently synthesized in a pure form (13). This zeolite exhibits a more open structure (14) and a higher Si/Al ratio, leading to a stronger acidity than the Y zeolite (15). Two series of catalysts were prepared depending on whether the molybdenum phase was supported on the sodium-form zeolite or on the ammonium-form zeolite.

The catalytic properties of these compounds for the *n*-heptane conversion will be compared to those of the bulk oxynitride phase (crystallographic type γ-Mo_2N) and of the HEMT zeolite.

An oxycarbonitride surface can be created on the oxynitride particles by the H_2/hydrocarbon feed mixture. In order to complete our comparison, we have studied the catalytic properties of bulk molybdenum oxycarbide (crystallographic type α-Mo_2C).

2. EXPERIMENTAL

2.1. Catalyst Preparation

By using a slightly modified procedure based on that of Delprato *et al.* (13), the NaEMT zeolite (Si/Al = 3.8, $S_g = 670\ m^2 \cdot g^{-1}$) was synthesized in a pure form. The partially NH_4^+ exchanged-EMT zeolite (denoted as NH_4EMT) was obtained by ion exchange at room temperature, using 5 g NaEMT suspended in 50 ml ammonium acetate solution ($1\ mol \cdot L^{-1}$). The experiment was repeated three times, leading to a degree of ion exchange ca. 75% for NH_4^+. The protonic form, denoted as HEMT, was generated by a thermal treatment at 773 K under flowing hydrogen

[1] To whom correspondence should be addressed. Fax: (33) 1 44 27 60 33. E-mail: jmm@ccr.jussieu.fr.

0021-9517/97 $25.00

(720 ml · h^{-1}). MoO_3 (Aldrich, 99,998%) was used as the precursor of the molybdenum oxynitride (MoO_xN_y) and of the molybdenum oxycarbide (MoO_xC_y). The volume hourly space velocity (VHSV) was about 10,000 h^{-1}. Bulk molybdenum oxynitride was prepared from MoO_3 powder in pure flowing ammonia. The temperature was increased linearly in three steps, first rapidly from 293 to 423 K (1 K · min^{-1}) and held at 423 K for 1 h, then from 423 to 623 K, and finally slower (0.5 K · min^{-1}) from 623 to 973 K. The temperature was held at 973 K for 4 h. The system was then cooled to room temperature (RT) in flowing ammonia, flushed with argon, and passivated for 1 h by 1 vol% O_2 in Ar (VHSV of 15,000 h^{-1}). Molybdenum oxycarbide was prepared from MoO_3 powder in 1/4 CH_4–H_2 mixture. The heating rates and temperatures used are identical to those described for molybdenum oxynitrides.

The chemical vapor phase deposition (CVD) of $Mo(CO)_6$ was used to prepare a first series of supported catalysts (0.5 to 1 g). The zeolitic support was first evacuated in high vacuum for 2 h at 423 K. Then according to the procedure described by Gallezot *et al.* (16), a suitable amount (5 wt% Mo/dry zeolite) of $Mo(CO)_6$ was evaporated onto the dehydrated EMT zeolite. Nitridation of the Mo-loaded samples was carried out by linearly increasing the sample temperature (1 K · min^{-1}) under a partial pressure of ammonia (300 Torr) from RT to 423 K. After 1 h at 423 K, flowing NH_3 (6 L · h^{-1}) was introduced and the temperature kept at 423 K for 1 h. Then the temperature was linearly increased from 423 to 973 K (1 K · min^{-1}) and held 4 h at 973 K. After the system was cooled to RT, it was purged with helium to remove ammonia. Passivation was made by slow contacting with the air.

The second method used to deposit the molybdenum in the zeolite porosity was a solid-state reaction which consisted in grinding finely dispersed powders of the hydrated zeolite and oxide (MoO_3) to mix them intimately (17). To facilitate the diffusion of the oxide into the zeolite porosity, a calcination under air was necessary prior to nitridation.

Molybdenum was also loaded with a third technique (incipient wetness impregnation) by filling the zeolite pores with an ammonium heptamolybdate solution of appropriate concentration.

The nitridation of these Mo-loaded samples was carried out as previously described for bulk molybdenum oxynitrides. They were passivated by flowing 1% O_2/Ar (v/v) mixture. The samples were denoted as follows: *w*-MoON-*T*/*z*EMT, where *w* is route 1, 2, or 3 for the loading methods of chemical vapor deposition, solid-state reaction, or wetness impregnation, respectively; MoON represents the molybdenum oxynitride which may be the oxynitride species; *T* is the Kelvin temperature of the ammonia treatment; and z = Na, NH_4, or H according to whether the zeolite was the sodium-, ammonium-, or protonic-form EMT, respectively.

2.2. Catalyst Characterization

The elemental analysis of the solids was obtained from the Service Central d'Analyse du Centre National de la Recherche Scientifique (Vernaison, France).

A Siemens D500 automatic diffractometer with a Cu$K\alpha$ monochromatized radiation source was used for the X-ray diffraction (XRD) patterns of the various solid phases. The degrees of X-ray crystallinity of the loaded zeolites were estimated from the intensity of all reflections in the range $2\theta = 14.5$–29.3° (18) and compared with those of the calcinated NaEMT zeolite. For the catalysts containing molybdenum species, the measured crystallinity had to be corrected (19) to assess the crystallinity of the EMT fraction.

The total specific surface areas (S_g) of the catalysts were obtained from the nitrogen desorption at different partial pressures by means of the BET method. A Quantasorb Jr. dynamic sorption system linked to a thermal conductivity detector was used. For S_g determination the materials were pretreated by heating in nitrogen at 373 K for 1 h then at 673 K for 3 h. Standard S_g measurements are based on a three-point analysis consisting of mixtures of 10, 20, and 30% N_2/He (v/v). The S_g values are reproducible within ±2%.

HRTEM studies of the catalysts were performed on a JEOL apparatus (JEM 100 CXII) equipped with a top entry device and operating at 100 kV. Ultramicrotome cuts (80–100 nm) of the samples were prepared for such studies. EDX analyses (STEM mode) were obtained from another JEM 100 CXII using a LINK AN 10000 system connected to a silicon–lithium diode detector and a multichannel analyzer. The EDX analyses were obtained either from relatively large domains of the samples (150×200 nm^2 to 400×533 nm^2) or from smaller domains (fixed STEM beam analysis 710 or 3000 nm^2).

The *n*-heptane isomerization/cracking reaction was carried out over 70 mg of catalyst in a flow reactor at 623 K and at a total pressure of 1 bar. The reaction feed was a mixture of hydrogen and *n*-heptane in a molar ratio of 17 to 1, the total gas flow being 0.7 L · h^{-1}. The samples were first pretreated at 773 K under flowing hydrogen for 5 h and then cooled to 623 K. The protonic form zeolite was generated from the ammonium form by the previous *in situ* pretreatment, leading mainly to a Brønsted acidity. The products of reaction were separated and identified by an on-line HP chromatograph, equipped with a 50-m PLOT capillary column coated with KCl-deactivated alumina and a FID detector.

3. RESULTS

3.1. Catalyst Characterization

For the elemental chemical analysis, passivated molybdenum oxynitrides and oxycarbides were pretreated in

TABLE 1

Characteristics of the Support of the Catalysts and Supported Materials

Samples	Theor. Mo loading (%)	Chemical analysis Mo/(Na + NH_4)	DRX cryst.[a] (%)	S_{BET} ($m^2 \cdot g^{-1}$)
NaEMT	—	—/Na_{20}	100	670
1-MoON-973/NaEMT	5	$Mo_{3.4}/Na_{20}$	104	603
1-MoON-723/NaEMT	5	$Mo_{3.2}/Na_{20}$	103	—
1-MoON-523/NaEMT	5	$Mo_{3.2}/Na_{20}$	102	—
NH_4EMT	—	—/(Na_5 + $(NH_4)_{15}$)	106	645
2-MoON-973/NH_4EMT	5	$Mo_{3.1}$/(Na_5 + $(NH_4)_{15}$)	56	370
3-MoON-973/NH_4EMT	6	$Mo_{4.2}$/(Na_5 + $(NH_4)_{15}$)	65	505
1-MoON-973/NH_4EMT	5	$Mo_{3.2}$/(Na_5 + $(NH_4)_{15}$)	105	590
1-MoON-723/NH_4EMT	5	$Mo_{2.2}$/(Na_5 + $(NH_4)_{15}$)	115	—
1-MoON-523/NH_4EMT	5	$Mo_{2.6}$/(Na_5 + $(NH_4)_{15}$)	109	—

[a] Crystallinity corrected from atomic absorption by the Mo phase for the supported materials.

vacuum at 773 K. Chemical formulae corresponding respectively to $MoO_{0.7}N_{0.9}$ (124 $m^2 \cdot g^{-1}$) and $MoO_{0.3}C_{0.7}$ (10 $m^2 \cdot g^{-1}$) indicated a high amount of oxygen in both cases. The atomic ratio metal/(N + O) for the oxynitride is far from the required ratio for a fcc structure. Undoubtedly there is a lack of molybdenum in the metal fcc sublattice. This has been observed by Gouin *et al.* (20) from density measurements. For each supported sample (Table 1), about 5 wt% Mo were loaded on the dry EMT zeolite. The high oxygen content of the zeolitic support precluded any possibility of distinguishing between the oxygen of the molybdenum species and that of the aluminosilicate support. XPS data (21) for $Mo(CO)_6$/NaEMT and $Mo(CO)_6$/NH_4EMT heated under flowing ammonia at different temperatures led us to the same conclusion as the O 1*s* binding energy (BE) of the support (about 532 eV) overlapped the BE of the bulk molybdenum oxynitride (530.5 and 532.6 eV).

For the solid–solid reaction (route 2), the zeolite–MoO_3 mixture was calcinated in flowing air to 773 K, allowing the oxide diffusion into the zeolite porosity (17, 22). As shown in Fig. 1, the MoO_3 diffraction peaks vanished after calcination at raising temperature (Figs. 1a to 1d), while chemical analysis revealed that molybdenum still remained. For this calcinated sample subsequently nitrided (2-MoON-973/NH_4EMT, Fig. 2b), only the X-ray diffraction pattern of zeolite is observed. The samples obtained by the same route, but directly nitrided without previous calcination led to some new X-ray diffraction peaks (asterisks in Fig. 2a) identified as those of the gamma phase of molybdenum nitride (JCPDS 25-1366) together with the EMT diffraction pattern. Consequently the formation of molybdenum oxynitrides aggregates outside of the zeolite can be assumed owing to the size of their particles.

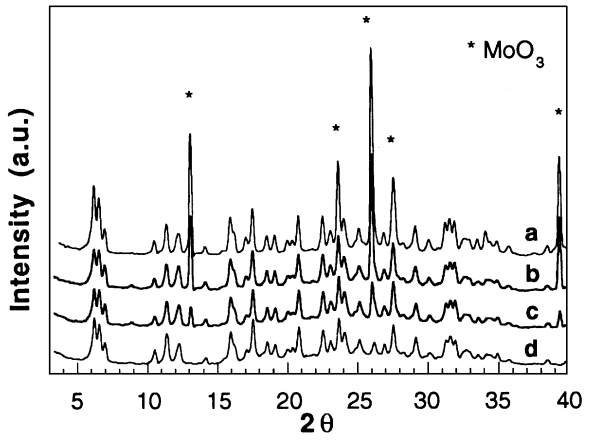

FIG. 1. Evolution of MoO_3–NH_4EMT mixtures (5 wt%) diffractograms according to calcination temperature: before calcination (a) and calcinated at 673 K (b), 723 K (c), and 773 K (d).

Concerning the samples prepared by impregnation (route 3), a calcination before nitridation by ammonia did not allow for a better introduction of the Mo phase inside the EMT cavities in comparison with no precalcination. XRD peaks characteristic of γ-Mo_2N also appeared but to a lesser extent than for the samples prepared by route 2 directly nitridated. From now on, for catalytic studies, compounds (3-MoON-973/NH_4EMT) directly nitrided will be used. A STEM image of this catalyst is shown in Fig. 3. The EMT grain can be seen in Fig. 3 as well as some stick-shaped particles located outside the zeolite. These sticks have in fact resulted from the aggregation of spherical particles ($d_p \approx 125$ Å). Selected area electron diffraction patterns permitted the identification of these nodules as γ-Mo_2N crystallites in agreement with X-ray diffraction data. EDX analysis, carried out on apparently clean zeolite areas, nevertheless detected the presence of a molybdenum phase

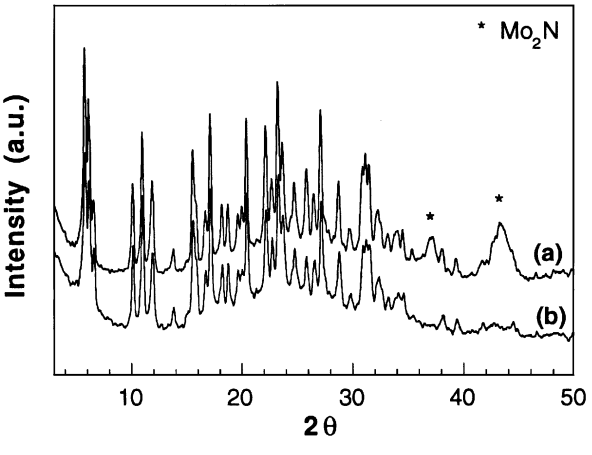

FIG. 2. Diffractograms of MoO_3–NH_4EMT mixture (5 wt%) after nitridation (973 K, flowing NH_3): (a) without precalcination; (b) with previous calcination (773 K, flowing air).

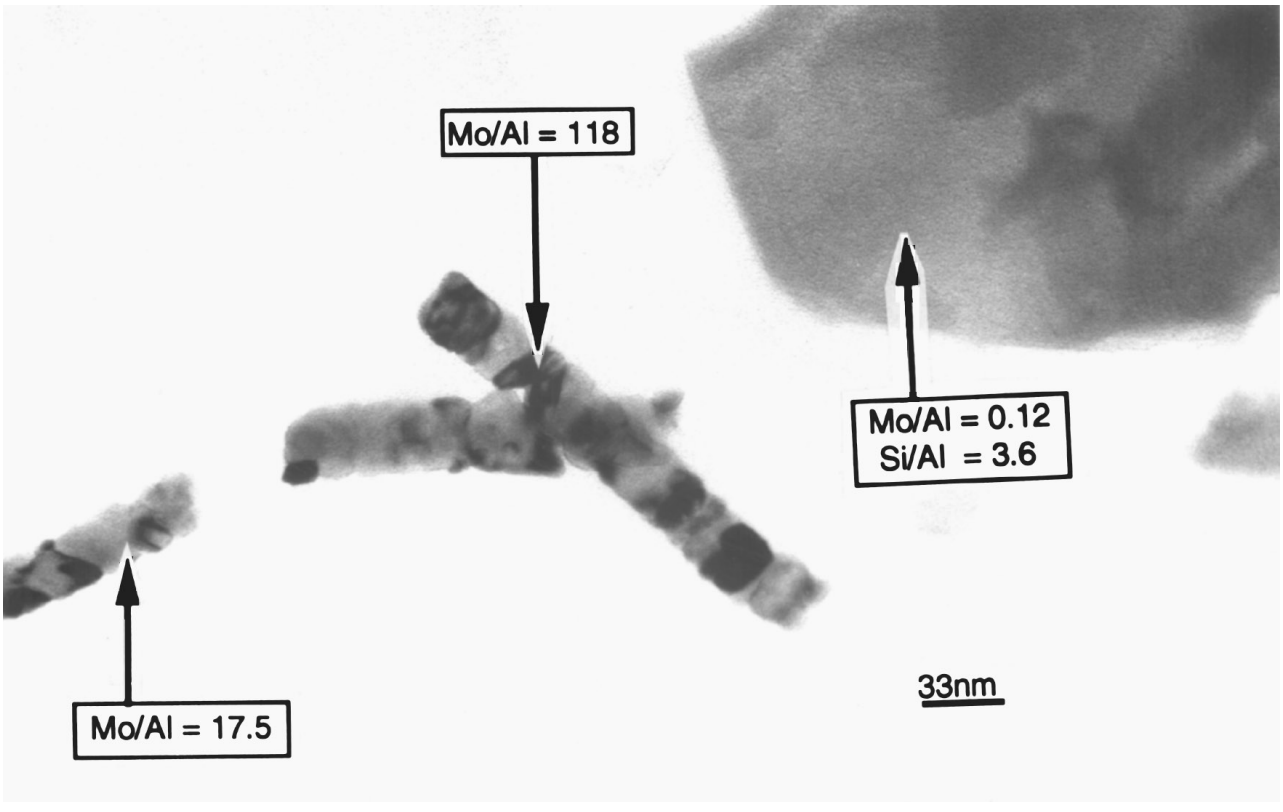

FIG. 3. STEM micrograph of thin cuts in 3-MoON-973/NH_4EMT sample.

homogeneously dispersed in the EMT porosity. Nine EDX measurements were performed on different zeolite areas (microtomic cuts) and the results gave an average atomic ratio Mo/Al = 0.12 with a low standard deviation (0.02). This value represents 60% of the molybdenum initially introduced by impregnation.

For samples prepared by chemical vapor deposition (route 1), a homogeneous distribution throughout the zeolite (EDX measurements on thin cut sections) and an ultradispersion ($d_p < 10$ Å) of the molybdenum phase were obtained (21). For these samples, 1-MoON-973/(NH_4EMT or NaEMT), X-ray diffraction pattern never showed diffraction lines of molybdenum oxynitride or oxycarbide. No particles greater than 10 Å in diameter could be observed by HRTEM inside or outside the zeolite grains, confirming the X-ray data for these compounds.

To determine the crystallinity of the support related to NaEMT, the XRD are corrected from the X-ray absorption by the Mo phase; the results are reported with the specific surface areas in Table 1. For synthesis by solid–solid reaction (route 2, calcination and nitridation) or by impregnation (route 3) directly followed by a nitridation (with no previous calcination), a noticeable decrease in crystallinity is observed. The evolution of the S_g values (645, 505, 370) is linked to the lowering of crystallinity (106, 65, 56, respectively).

On the contrary, the chemical vapor deposition allowed us to prepare some molybdenum oxynitride-loaded catalysts with no decrease of the zeolite crystallinity (100 for NaEMT and about 100 for all other route-1 compounds). But the specific surface area decreased substantially (within experimental error) due to the location of molybdenum species in the cavities. Nevertheless for the various catalysts, the unit-cell parameters of the molybdenum oxynitrides-loaded EMT zeolite were practically unchanged after loading with Mo and nitridation.

3.2. Catalytic Behavior

3.2.1. Molybdenum Oxynitrides Supported on an Inert NaEMT Zeolite

In this section, data on the 1-MoON-*T*/NaEMT catalysts ($T = 973$, 723, or 523 K) in the *n*-heptane conversion will be considered and compared to those obtained from bulk molybdenum oxynitride and oxycarbide. Selectivities were defined as a fraction of 100 moles of *n*-heptane converted and are reported in Table 2 as well as the distribution of the products for each kind of reaction (moles for 100 moles of products from isomerization, hydrogenolysis, dehydrogenation, or aromatization). With the bulk molybdenum compounds and the MoON-loaded NaEMT catalysts, isomerization was the most significant reaction

TABLE 2

Selectivity and Distribution of Products for the *n*-Heptane Reaction at 623 K after 6 h on Stream

Samples	Conv. (%)	Isomerization Isoheptanes (%) 2m 3m	2,4 dm	Et	Dehyd. C7=	Arom. Toluene	Hydrogenolysis Light products (%) C1 + C6	C2 + C5	C3 + C4
MoO_xN_y bulk	4		75.1		3.7	1.8		20.4	
		96.1	1.6	2.3			16.3	39.7	43.9
1-MoON-973/NaEMT	1.3		55.6		22.1	—		22.3	
		85.1	—	14.9			20.0	24.4	55.6
1-MoON-723/NaEMT	2		73.5		15.4	—		11.1	
		90.0	2.3	7.7			29.8	20.5	49.7
1-MoON-523/NaEMT	3		76.9		8.9	—		14.2	
		93.4	2.4	4.2			23.2	22.2	54.6
MoO_xC_y bulk	4.6		54.8		3.5	3.5		38.2	
		96	2.2	1.8			44.8	30.1	25.1

Note. Conv., total conversion; Dehyd., dehydrogenation; Arom., aromatization; 2m 3m, 2-methyl- and 3-methylhexanes; 2,4 dm, 2,4-dimethylpentane; Et, ethylpentane; C7=, heptenes.

leading predominantly to methylhexane isomers. Products of cracking/hydrogenolysis (C1–C6) or dehydrogenation (heptenes) were always present in small amounts except for molybdenum oxycarbide. Compared to the molybdenum oxynitrides supported on NaEMT, this latter compound favored the hydrogenolysis products against the dehydrogenated ones more strongly. For the bulk molybdenum oxynitride, it can be seen that the *n*-heptane conversion did not vary with time-on-stream as for the reaction performed over the 1-MoON-*T*/NaEMT catalysts (Fig. 4).

To determine the number of accessible sites, we assumed a stoichiometric fcc lattice structure and a density of about 10^{15} Mo atoms/cm^2 was generally considered for bulk oxynitrides. For the supported catalyst (route 1), the molybdenum species were supposed to be 100% dispersed (particle diameter less than 10 Å). It was thus possible to calculate the rate for the *n*-heptane conversion and the product formation rates as a site time yield (STY) in our conditions. STY was defined as the number of molecules produced in a catalytic bed per second per surface metal atom (23). Table 3 reports the *n*-heptane reactions and dehydrogenation (as heptenes) site time yields for bulk molybdenum oxynitride and supported catalysts obtained via route 1.

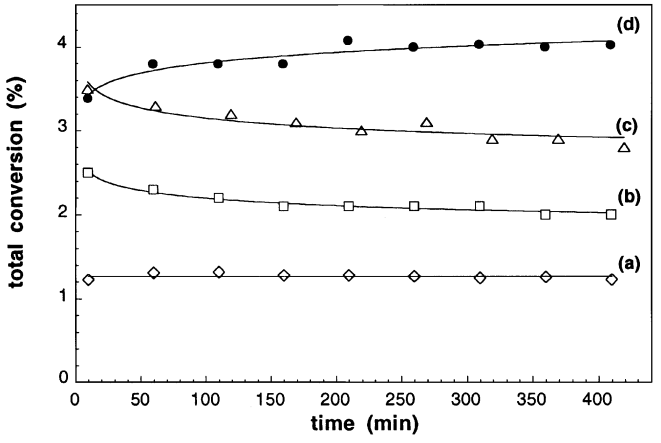

FIG. 4. Evolution of total conversion of *n*-heptane according to time on stream over 1-MoON-973/NaEMT (a), 1-MoON-723/NaEMT (b), 1-MoON-523/NaEMT (c), and bulk MoO_xN_y (d).

3.2.2. *Molybdenum Oxynitrides Supported on an Acidic HEMT Zeolite*

In this section, data on the *x*-Mo N-*T*/HEMT catalysts in the *n*-heptane conversion will be presented and compared to those obtained with an unloaded HEMT zeolite. The protonic form of the zeolite was generated by treatment at 773 K under hydrogen of loaded or unloaded NH_4EMT.

Effect of oxynitrides on n-heptane reactions over loaded HEMT zeolite. The activity at 623 K of each catalyst versus time-on-stream is represented in Fig. 5 and it can be seen that the conversion is higher when a molybdenum nitride phase is loaded. A significant deactivation is

TABLE 3

***n*-Heptane Reaction and Dehydrogenation (as Heptene) Site Time Yield (STY) at 623 K after 6 h on Stream (Steady State Condition)**

Samples	MoO_xN_y bulk	1-MoON-973/NaEMT	1-MoON-723/NaEMT	1-MoON-523/NaEMT
n-Heptane reaction STY (10^4 s^{-1})	1.5[a]	1.7[b]	3.3[b]	5.0[b]
Dehydrogenation STY (10^4 s^{-1})		0.4[b]	0.5[b]	0.4[b]

[a] Calculated with a 10^{15} sites · cm^{-2} active site density assumption.
[b] Calculated assuming a 100% fraction exposed of metallic atoms.

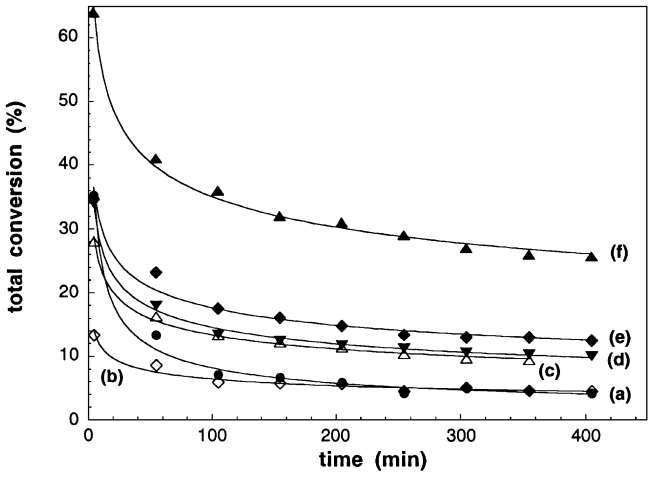

FIG. 5. Evolution of *n*-heptane total conversion according to time on stream for HEMT (●, a) and supported catalysts: 2-MoON-973/HEMT (◇, b), 3-MoON-973/HEMT (△, c), 1-MoON-973/HEMT (▼, d), 1-MoON-723/HEMT (◆, e), and 1-MoON-523/HEMT (▲, f).

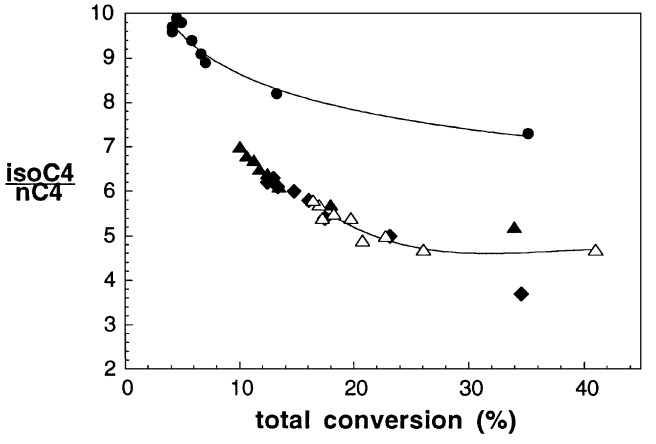

FIG. 6. Evolution of *iso*-C4/*n*-C4 ratio according to conversion level for HEMT-based catalysts (due to catalyst deactivation conversion varies): HEMT (●), 1-MoON-973/HEMT (▲), 1-MoON-723/HEMT (◆), and 1-MoON-523/HEMT (△).

observed for each catalyst but more rapidly for HEMT (Fig. 5a) compared to loaded catalysts. The activity decay is well described by the Voorhies equation $A = A_1 \cdot t^{-n}$ (24), where A_1 is the activity after 1 min reaction, n the deactivation constant, and t the time of run. A_1 and n were deduced by linearization (log A vs log t, correlation coefficient systematically better than 0.995). The term A is directly related to the conversion and is expressed in molecules $\cdot\, h^{-1} \cdot$ (acid sites)$^{-1}$, assuming that the acid site number by unit cell is equal to the ammonium group number in the zeolite framework. V_{res} is the residual specific rate after 350 min on stream, expressed in mol $\cdot\, h^{-1} \cdot (g_{cata})^{-1}$, when a quasi-steady state is reached. Table 4 lists the calculated constants for the Voorhies equation together with the crystallinity evaluated after a catalytic pretreatment at 773 K under flowing hydrogen.

Study of the distribution of the reaction products. The catalytic activities of the HEMT-based catalysts are given in Table 5 for a nearly identical conversion. For all catalysts, cracking was the most significant reaction; however, the formation of *n*-heptane isomers could be observed. At the beginning of the reaction, propane and isobutane constituted the main cracking products, while isomerization consisted mainly of methylhexanes. Traces of ethane and toluene were also observed. Branched-to-linear C4 ratio always presented a high value from 7 to 10 after 340 min on stream, significantly exceeding the thermodynamic value (0.8 at 623 K). As can be seen in Fig. 6, this *iso*-C4/*n*-C4 ratio is always high in comparison with the thermodynamic value for the loaded HEMT compounds (between 7 and 4) but this ratio remained lower than observed with the HEMT. In Fig. 7, it can also be observed that the paraffin/olefin ratio (C3 fraction) is about two or three times greater for loaded HEMT than for unloaded HEMT zeolite.

TABLE 4

Evolution of the Voorhies Equation Constants with the Preparation Mode or the Sample Nitridation Temperature

	$A = A_0 \cdot t^{-n}$			
Catalysts	A_1 (mol $\cdot$ h^{-1} $\cdot$ (OH-sites)$^{-1}$)	n	V_{res} (mol $\cdot$ h^{-1} $\cdot$ g^{-1})	Crystallinity (%)
HEMT	5.9	0.44	1.3×10^{-3}	105
2-MoON-973/HEMT	3.3	0.34	1.4×10^{-3}	55
3-MoON-973/HEMT	4.2	0.26	2.8×10^{-3}	60
1-MoON-973/HEMT	5.2	0.28	3.0×10^{-3}	97
1-MoON-723/HEMT	5.3	0.24	3.9×10^{-3}	112
1-MoON-523/HEMT	9.1	0.21	7.6×10^{-3}	106

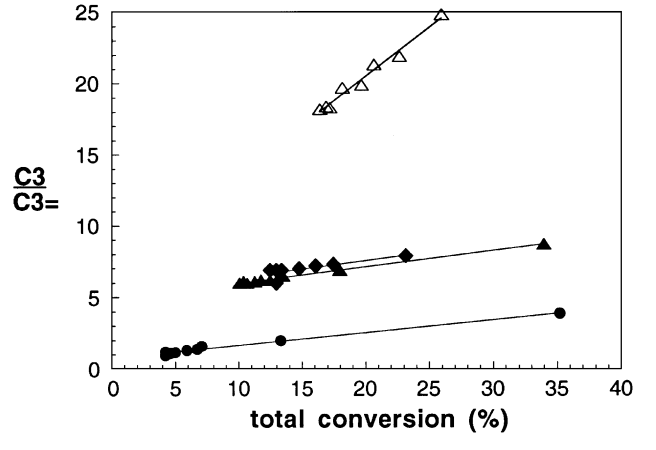

FIG. 7. Evolution of paraffin/olefin ratio according to conversion level for supported or unsupported HEMT catalysts for the C3 fraction (due to catalyst deactivation conversion varies): HEMT (●), 1-MoON-973/HEMT (▲), 1-MoON-723/HEMT (◆), 1-MoON-523/HEMT (△).

TABLE 5

Selectivity and Distribution of Products for *n*-Heptane Isomerization/Cracking Reactions at 623 K for Supported HEMT Catalysts at an Equivalent Conversion Percentage

Catalysts	Conv. (%)	Isomerization Isoheptanes (%)			Arom.	Crac.	Light products (%)										
							C3		C4			C5			C6		
		2m 3m	2,3 dmP	EtP	Toluene		C3	C3=	*n*	iso	C4=	*n*	iso	C5=	*n*	iso	cyc
HEMT	**13.3**		**3.9**		**0.8**	**95.3**	45.2			48.0			5.2			1.6	
		91.2	8.8	—			66.8	33.2	9.9	81.1	9	7.8	72.1	20.1	6.2	59.5	34.3
1-MoN-523/HEMT	**16.5**		**7.5**		**0.5**	**92**	50.2			47.3			1.7			0.8	
		85.6	9.3	5.1			94.8	5.2	14.3	82.8	2.9	—	76.3	23.7	—	44.5	55.5
1-MoN-723/HEMT	**13.4**		**4.5**		**0.8**	**94.7**	49.8			47.0			2.4			0.8	
		90.9	9.1	—			87.3	12.7	13.4	82.8	2.9	5.4	94.6	—	—	100	—
1-MoN-973/HEMT	**13.5**		**4.1**		**0.7**	**95.2**	49.6			46.3			3.0			1.1	
		90.9	9.1	—			86.7	13.3	13.6	82.1	4.3	6.9	93.1	—	16.4	83.6	—
3-MoN-973/HEMT	**13.3**		**6.1**		**0.7**	**93.2**	49.8			46.1			3.1			1.0	
		85.1	7.1	7.8			93.7	6.3	17.4	78.1	4.5	6.3	93.7	—	24.1	75.9	—
2-MoN-973/HEMT	**13.3**		**1.8**		—	**98.2**	49.4			45.3			4.3			1.0	
		100	—	—			80.4	19.6	13.8	76.5	9.7	20.6	77.4	2.0	22	26.6	51.4

Note. Conv., total conversion; Arom., aromatization; Crac., cracking; 2m 3m, 2-methyl- and 3-methylhexanes; 2,3 dmP, 2,3-dimethylpentane; EtP, ethylpentane; C*x*, paraffin; C*x*=, olefin; *n*, *n*-paraffin; iso, isomers: cyc, cyclic paraffin (*x* represents the carbon atom number). The selectivity for a type of reaction is calculated in fractions of 100 moles of *n*-heptane converted (bold type). The distribution of products for each type of reaction is expressed in moles for 100 moles of products obtained in isomerization, cracking, or aromatization.

3.3. Discussion

3.3.1. Preparation Routes and Reactivity

Various modes of preparations permitted us to obtain molybdenum oxynitrides dispersed on EMT zeolite. It was shown that when the molybdenum species was inside the zeolite porosity, it was dispersed in the form of small aggregates lower than 10 Å in diameter. No sintering of these clusters occured after nitridation. Nevertheless a substantial decrease of the crystallinity of the support was observed after the solid-state reaction (Table 1), this loss being more important after grinding and calcination followed by a subsequent nitridation. Fraissard *et al.* (25) reported such lattice destruction during MoO_3 migration during calcination, in the NaY porosity with a higher concentration (two times greater). They observed the complete diffusion of MoO_3 into the channels or supercages of the zeolite for the same calcination temperature (750 K) and assumed this insertion was due to the low melting point and solubility of MoO_3 in hot water. A zeolite crystallinity decay was also observed for 3-MoON-973/NH_4EMT (route 3) for which 60% of the molybdenum loaded was found to be inside the zeolite porosity by EDX and chemical analysis. Thus, it seemed that an interaction between the molybdenum oxide and the zeolite was responsible for the EMT collapse during this route 3 since no decrease of the zeolite crystallinity was observed when $Mo(CO)_6$ was used as a precursor (route 1). As a conclusion for the supported HEMT catalysts, the preparation mode played an important role to preserve the zeolite crystallinity.

The reactivity of these catalysts in the *n*-heptane conversion was a good probe to check the physicochemical state of the solid (crystallinity and dispersion of the molybdenum species). The following conclusions can be drawn:

—the *n* Voorhies constant being the deactivation parameter, a low value of *n* indicates the molybdenum phase hydrogenating capacity.

—The evolution of V_{res} (residual specific rate after 350 min on stream) depends on both the deactivation and the crystallinity of the zeolite. The higher the V_{res}, the lower the deactivation and the higher the accessibility of the hydrogenating sites linked to the crystallinity of the support. The best routes can be described as

1-MoON-973/NH_4EMT > 3-MoON-973/NH_4EMT > 2-MoON-973/NH_4EMT

Let us consider route 1 for 1-MoON-*T*/NH_4EMT; it can be seen that the lower the nitridation temperature, the higher the reactivity. For all these catalysts, as they have the highest possible crystallinity, the increase of the temperature of preparation only decreased the molybdenum-phase dispersion as seen by the highest deactivation (*n* values, Table 4). Similarly, for the NaEMT-supported catalysts, the

1-MoON-523/NaEMT presents a higher STY value for the *n*-heptane reactions than the 1-MoON-973/NaEMT.

3.3.2. The Hydrogenating Function of the Supported Molybdenum Oxynitride

(a) Molybdenum species supported on NaEMT zeolite, a nonacidic support, behave like a bulk MoO_xN_y with predominantly the isomerization of the *n*-heptane to methylhexanes and similar site time yields (Table 3). It was further checked by XPS measurements that the bulk molybdenum phase was a molybdenum oxynitride containing a significant amount of oxygen (atomic ratio O/Mo = 0.4) before passivation, with about 75% of these oxygen atoms being implied in an oxide-like bond (BE = 530.4 eV) (21). This type of oxygen is able to create weak Brønsted acidic sites and provides bifunctional properties to the molybdenum oxynitride leading to isomerization (26). The dehydrogenation STY (*n*-heptane to heptenes) (route 1) of the supported catalysts are remarkably independent from the temperature of synthesis (Table 3). These results suggest that the densities of active metallic sites responsible for the formation of dehydrogenation products are similar for the three supported catalysts. It is thus conceivable that supported molybdenum species behave like bulk MoO_xN_y since they exhibit almost the same selectivity and STY in *n*-heptane reactions (Table 3). Furthermore, if a number of product molecules is calculated for each class of reaction from Table 2 (conversion × selectivity), it can be pointed out that the decrease of the total conversion with increasing temperature was mainly due to the decrease of isomerization. A higher temperature of preparation decreases the density of acidic sites required for an isomerization according to a bifunctional sequence. It can thus be considered that the ratio acidic/metallic functions decreased when the temperature of preparation increased, that is, with oxynitride particles probably containing less oxygen. The distribution of the products given in Table 2 showed that 1-MoON-523/NaEMT (5 wt% Mo) behaves like the bulk oxynitride for both *n*-heptane isomerization (75 and 76.9%, respectively, with a selectivity exceeding 95% mainly toward monobranched isomers) and hydrogenolysis (20.4 and 14%, respectively).

In our case, we cannot exclude the influence of a carbide layer formed by contact with the H_2/hydrocarbon feed mixture after time on stream. This possibility can explain the lowering of the isomerization level for the 1-MoON-973/NaEMT, molybdenum oxycarbide favoring hydrogenolysis against isomerization. A carbide phase activated by air at 623 K and referenced as $Mo_2C{-}O_{623}$ has been described by Ledoux *et al.* (27). This bulk material is supposed to be an oxygen-defective MoO_3 structure with carbon filling some of the vacancies. Before catalytic use, the carbide was oxidized in a stream of flowing air at 623 K for 14 h in order to activate the carbide. The oxidative treatment producing the oxidized catalyst leads to an active and selective catalyst in isomerization of *n*-heptane. A conversion rate of 3×10^{-7} mol · g^{-1} · s^{-1} was reached after 4 h at 623 K, STY calculated on this conversion rate assuming 10^{15} metallic site/cm^2 and 40 m^2/g for the oxidized carbide leads to a value of 4.2×10^{-4} s^{-1} near our values for *n*-heptane reactions.

(b) When molybdenum nitrides were supported on the acidic HEMT zeolite, cracking was the most significant reaction (92–95%), indicating that the strength of the zeolite acidic sites was quite higher than that of the molybdenum oxynitride. The highest paraffin/olefin ratio (Fig. 7) in the cracking products for the loaded HEMT confirms the significant hydrogenating function brought by the dispersed molybdenum oxynitrides. It explains how the dispersed phase acted to increase the conversion level or to decrease the deactivation rate. It is well known that deactivation of zeolite-based catalysts is mainly due to the formation of coke molecules blocking the active acid sites. These species should consist of molecules with 25–30 carbon atoms resulting from oligomerization of olefins (28, 29). Thus, by hydrogenating the unsaturated products of the *n*-heptane conversion, the molybdenum oxynitrides limited the coking and endowed the loaded catalysts with a longer lifetime. The presence of the oxynitride also favored the hydrogenation of the isoheptane carbenium ions and consequently facilitated their desorption before any cracking; it explained the decrease of the *iso*-C4/*n*-C4 ratio (Fig. 6). The supported catalysts acted then as bifunctional catalysts with a low hydrogenating/acidic site ratio (30).

4. CONCLUSION

Molybdenum oxynitrides were readily introduced into the EMT zeolite by several loading methods, the most efficient being the CVD of $Mo(CO)_6$ followed by nitridation. This mode of preparation prevented the zeolite crystallinity from decreasing due to the molybdenum oxide interactions with the zeolite. When inserted into the EMT porosity, the molybdenum containing phase was homogeneously dispersed throughout the zeolite grain and the particle diameters were less than 10 Å. According to *n*-heptane reactions, these materials behaved as bifunctional catalysts. Indeed, the MoON/NaEMT catalysts nearly matched the activity of the bifunctional bulk molybdenum oxynitride with similar selectivities in isomerization and equivalent site time yields for *n*-heptane reactions. Despite their satisfactory dispersion, the Mo oxynitrides loaded into the HEMT zeolite did not exhibit a sufficient hydrogenating capacity to induce a high selectivity for isomerization of heptane. Nevertheless, they acted in hydrogenating the unsaturated products of the reaction and were thus able to limit the formation of coke. Consequently, the cracking activity of the loaded HEMT catalysts was enhanced compare to that of the bare HEMT.

ACKNOWLEDGMENTS

The authors gratefully acknowledge Mrs. P. Beaunier and Mr. M. Lavergne for STEM-EDX and TEM measurements.

REFERENCES

1. Muller, J. M., and Gault, F. G., *Bull. Soc. Chim. Fr.*, 416 (1970).
2. Sinfelt, J. H., and Yates, D. C. F., *Nature Phys. Sci.* **229**, 27 (1971).
3. Levy, R. B., and Boudart, M., *Science* **181**, 547 (1973).
4. Ribeiro, F. H., Dalla Betta, R. A., Baumgartner, J., and Iglesia, E., *J. Catal.* **130**, 86 (1991).
5. Bell, A. T., Lee, K. S., Reimer, J. A., and Abe, H., *J. Catal.* **138**, 393 (1992).
6. Volpe, L., and Boudart, M., *J. Solid State Chem.* **59**, 332 (1985).
7. Oyama, S. T., Schlatter, J. C., Metcalfe, J. E. III, and Lambert, J. M., Jr., *Ind. Eng. Chem. Res.* **27**, 1639 (1988).
8. Jaggers, C. H., Michaels, J. N., and Stacy, A. M., *Chem. Mater.* **2**, 150 (1990).
9. Djega-Mariadassou, G., Boudart, M., Bugli, G., and Sayag, C., *Catal. Lett.* **31**, 411 (1995).
10. Nagai, M., and Miyao, T., *Catal. Lett.* **15**, 105 (1992).
11. Nagai, M., Miyao, T., and Tuboi, T., *Catal. Lett.* **18**, 9 (1993).
12. Colling, C. W., and Thompson, L. T., *J. Catal.* **146**, 193 (1994).
13. Delprato, F., Delmotte, L., Guth, J. L., and Huve, L., *Zeolites* **10**, 546 (1990).
14. Baerlocher, C., McCusker, L. B., and Chiappetta, R., *Microporous Mater.* **2**, 269 (1994).
15. Su, B. L., Manoli, J. M., Potvin, C., and Barthomeuf, D., *J. Chem. Soc. Faraday Trans.* **89**, 857 (1993).
16. Gallezot, P., Coudurier, G., Primet, M., and Imelik, B., *in* "Molecular Sieves II" (J. R. Katzer, Ed.), Vol. 40, p. 144. ACS Symposium Series, 1977.
17. Kucherov, A. V., and Slinkin, A. A., *Zeolites* **7**, 38 (1987).
18. Chatelain, T., Patarin, J., Soulard, M., Guth, J. L., and Schultz, P., *Zeolites* **15**, 90 (1990).
19. Léglise, J., Manoli, J-M., Potvin, C., Djéga-Mariadassou, G., and Cornet, J., *J. Catal.* **141**, 275 (1995).
20. Gouin, X., Marchand, R., L'Haridon, P., and Laurent, Y., *J. Solid State Chem.* **109**, 175 (1994).
21. Becue, T., Thesis, Université de Paris VI, Paris, 1996.
22. Karge, H. G., and Beyer, H. K., *Stud. Surf. Sci. Catal.* **69**, 43 (1991).
23. Boudart, M., Oyama, S. T., and Leclercq, L., *in* "Proceedings, 7th International Congress on Catalysis" (T. Seiyama and K. Tanabe, Eds.), Vol. 1, p. 578. Elsevier, Amsterdam. 1981.
24. Voorhies, A., *Ind. Eng. Chem.* **37**, 318 (1945).
25. Thoret, J., Marchal, C., Dorémieux-Morin, C., Man, P. P., Gruia, M., and Fraissard, J., *Zeolites* **13**, 269 (1993).
26. Iglesia, E., Baumgartner, J. E., Ribeiro, F. H., and Boudart, M., *J. Catal.* **131**, 523 (1991).
27. Blekkan, A., Pham-Huu, C., Ledoux, M., and Guille, J., *Ind. Eng. Chem. Res.* **33**, 1657 (1994).
28. Alvarez, F., Giannetto, G., Montes, A., Ribeiro, F., Pérot, G., and Guisnet, M., *Stud. Surf. Sci. Catal.* **37**, 479 (1988).
29. Pérot, G., Hilaireau, P., and Guisnet, M., *in* "6th International Zeolite Conference" (D. Olson and A. Bisio, Eds.), p. 427. Butterworth, London, 1984.
30. Guisnet, M., Alvarez, A., Giannetto, G., and Pérot, G., *Catal. Today* **1**, 415 (1987).